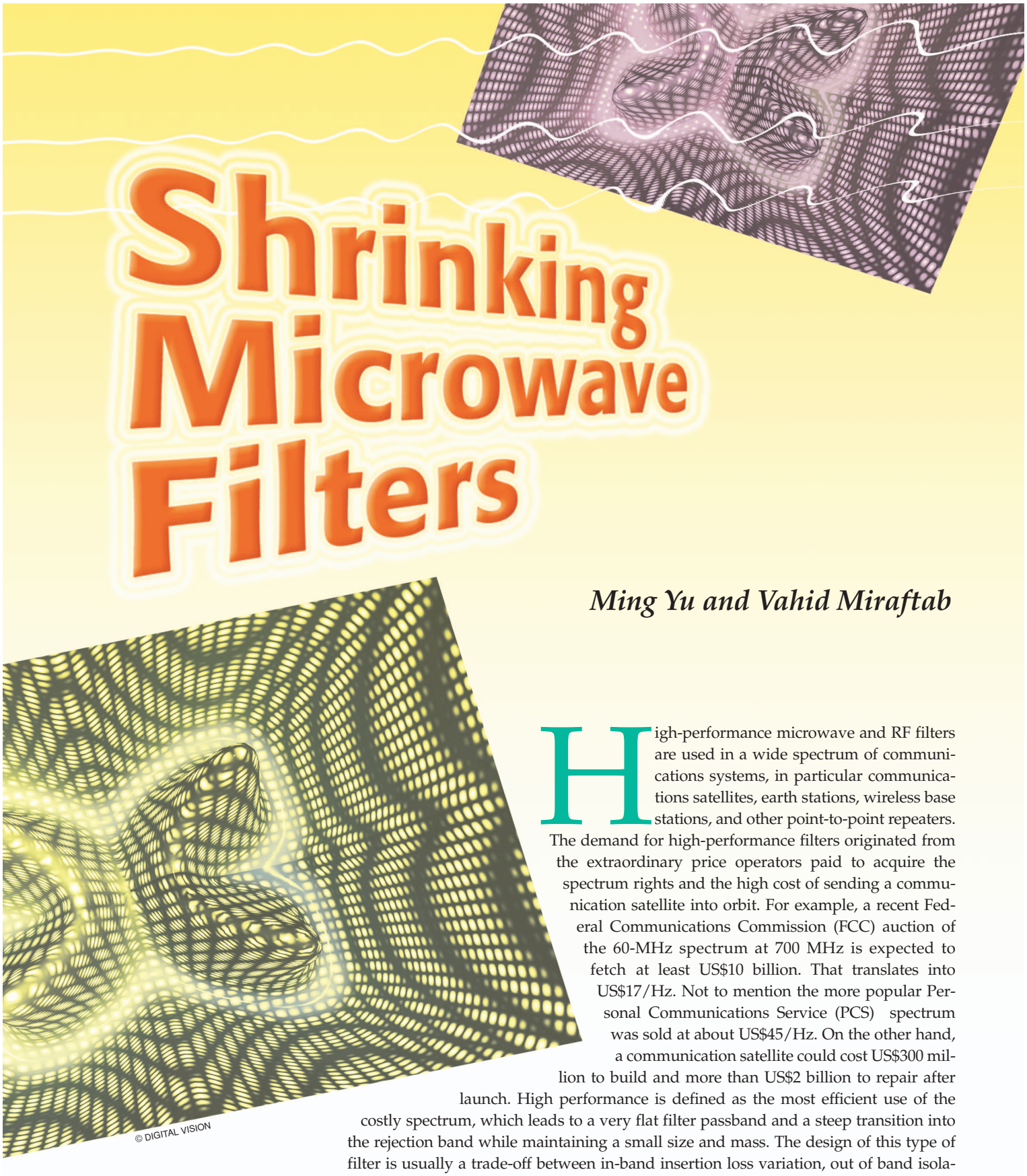

Shrinking Microwave Filters

Ming Yu and Vahid Miraftab

High-performance microwave and RF filters are used in a wide spectrum of communications systems, in particular communications satellites, earth stations, wireless base stations, and other point-to-point repeaters. The demand for high-performance filters originated from the extraordinary price operators paid to acquire the spectrum rights and the high cost of sending a communication satellite into orbit. For example, a recent Federal Communications Commission (FCC) auction of the 60-MHz spectrum at 700 MHz is expected to fetch at least US$10 billion. That translates into US$17/Hz. Not to mention the more popular Personal Communications Service (PCS) spectrum was sold at about US$45/Hz. On the other hand, a communication satellite could cost US$300 million to build and more than US$2 billion to repair after launch. High performance is defined as the most efficient use of the costly spectrum, which leads to a very flat filter passband and a steep transition into the rejection band while maintaining a small size and mass. The design of this type of filter is usually a trade-off between in-band insertion loss variation, out of band isolation (of course, other parameters such as absolute loss, group delay, and gain slope must

Ming Yu (ming.yu@ieee.org) and Vahid Miraftab are with COM DEV, 155 Sheldon Drive, Cambridge, Ontario, N1R 7H6, Canada.

Digital Object Identifier 10.1109/MMM.2008.927636

 1527-3342/08/$25.00©2008 IEEE

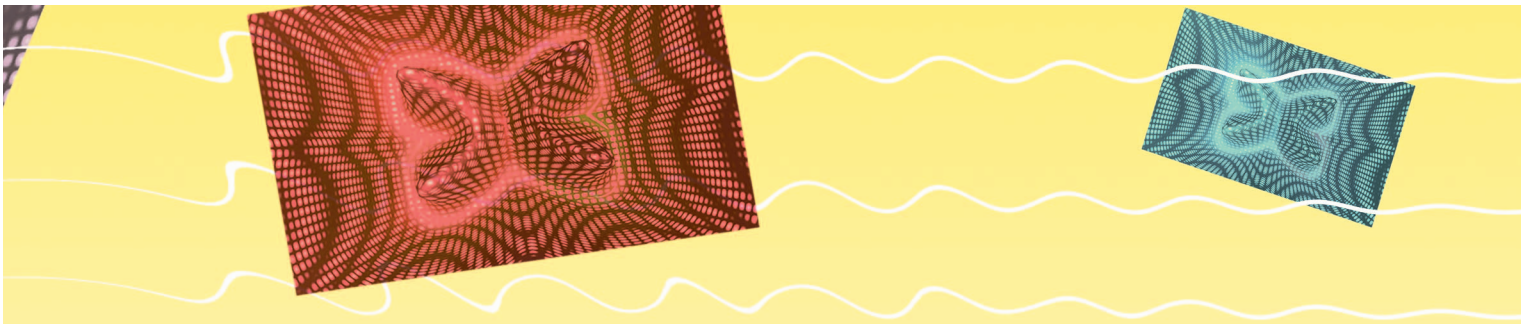

be part of the trade-off and are purposely omitted for the sake of simplicity), physical size, and mass. The approach of designing microwave filters using different functions—expressed often in polynomial form—is well documented [1]. Not so surprisingly, filter designers often find that very high quality factor (Q) is required in order to create high-performance filters. Once the material and type of resonator are chosen, the Q is unfortunately constrained. In order to increase the Q, one often must increase the size of the resonator (especially for high-power applications), resulting in a larger and heavier filter. The finite Q (highest possible value selected after the trade-off between size and performance is made) will translate to energy dissipation. The filter will also exhibit finite band-edge sharpness related to the particular Q value. This phenomenon is more pronounced for filters with narrow proportional bandwidth (typically $\leq$1%). When size and mass are also important design drivers, dielectric or high-temperature superconductor (HTS) resonators (planar) are the best known choices to maintain or even boost Q while reducing size and mass simultaneously (under certain conditions). The dielectric resonators are now widely used for both high- and low-power applications, while HTS technology (generally for low-power applications) did not take off commercially due to cost and risk factors associated with the extra cryogenic coolers.

Filters used in the low-power side of the system are the focus of this article, since it maybe possible to trade off insertion loss for better filter shape. Typically, they are used in the receive side after the low noise amplifier (LNA) for interference filtering and signal channelization as shown in Figure 1(a) and (b). One common application is the input multiplexer (IMUX) assemblies of communication satellite transponders shown in Figure 1(b), where a bank of filters is used to channelize the input spectrum. In both cases, absolute insertion loss value is no longer critical since the LNA can easily make up the loss of the filter by setting the gain to a higher value. High Q resonators were used for those applications solely to achieve sharper band edge rolloff. The most critical electrical parameters for an IMUX filter are in band performance (such as loss variation) and group delay. From a physical perspective, mass and volume are also very critical considerations. The absolute insertion loss in the band center is often a secondary parameter that can be traded for size reduction. An IMUX is incorporated in the payload after the LNAs, which are part of the RF receiver, and prior to the channel high-power amplifiers. The gain of the LNAs and/or channel amplifiers is programmable in most satellites. The IMUX loss, as long as it is not excessive, has no impact on the satellite G/T (figure of merit for receiving equipment).

For a conventional filter/amplifier cascade architecture shown in Figure 2(a), a low-loss filter is often placed before the LNA. Moving some selectivity requirement into the second filter is sometimes used to relax the requirement of the first filter. In recent years, a new approach emerged to split the amplifier into two stages as shown in Figure 2(b) with a higher loss, but with a better selectivity [2]. All the scenarios discussed above provide the motivation for this article: trading absolute insertion loss to reduce size and mass. At the

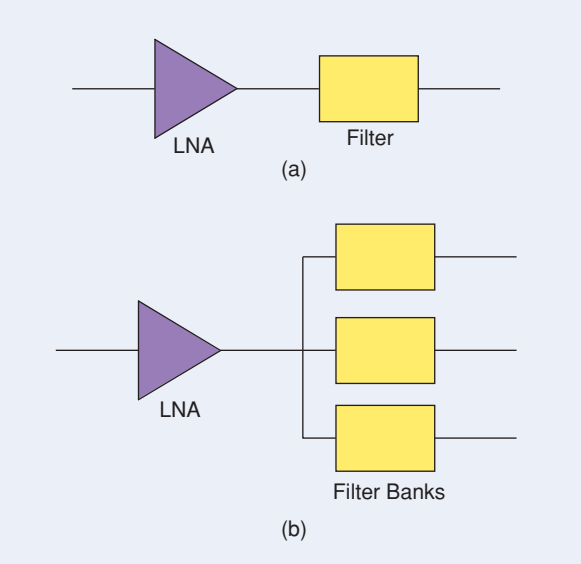

Figure 1. *Receive chain filters and channelization. (a) One channel receiver. (b) Multichannel receiver (IMUX).*

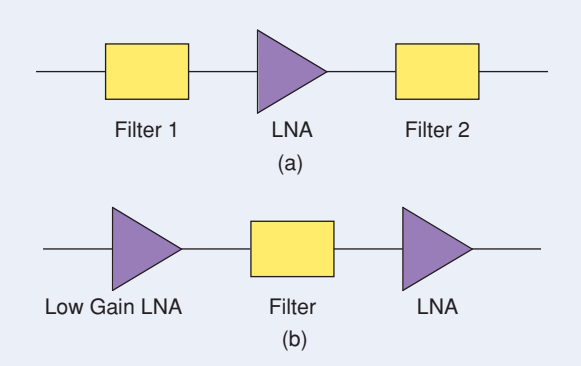

Figure 2. *Distributed filtering with (a) two filter stages and (b) two low noise amplifers.*

In order to reduce the size, we needed to find ways to use low Q resonators and make them behave like high Q resonators.

same time, it is also possible to enhance the performance or at least maintain similar performance by using lower Q resonators. The most promising approaches are adaptive predistortion [3], [4] and lossy circuit techniques [5], [6].

In the area of microwave filter design, the concept of predistortion was first proposed by Livingston [7] and later described in more detail by Williams [8] for cross-coupled microwave filters (with nonadjacent cavity couplings to realize transmission zeros). It is noted that they both attempted to predistort a relatively high Q filter and the approach did not change the size and weight of the filter. The goal of their contribution was to enhance the filter performance (loss variation) by emulating even much higher Q (in [8], $Q = 8{,}000$).

In search of the next technological advancement for the high-performance filters, we set the goal to reduce the mass and volume of the single-mode dielectric filter and cavity filters using dual mode while preserving the advantages and attributes of those filters. It is well known that the size and mass of filters are driven by the Q required. In order to reduce the size, we needed to find ways to use low Q resonators and make them behave like high Q resonators. This contribution makes full use of the possibility of insertion loss trade-off by applying an adaptive predistortion technique to a very low Q filter (<3,000). This approach not only improves the performance of the loss variation (with much smaller insertion loss penalty) but also reduces the size and mass significantly.

In this article, we demonstrate the feasibility of predistorted filters that can achieve an equivalent Q of >20,000, while providing more than a three-to-one reduction in mass and volume over current C-band single-mode dielectric resonator filters, yet only introducing an additional 4 dB of insertion loss. We also show that the same approach can be applied to Ku-band filters to improve the filter performance.

Another interesting characteristic of adaptively predistorted filters is that the reflection zeros are no longer on the jω axis, which leads to more than one solution. After careful examination, a symmetrical realization for adaptively predistorted microwave filters is deemed as the best solution. The new realization enables much simpler conversion from an existing nonpredistorted filter design. Hence, both design and tuning efforts are reduced. A 10-4-4 dielectric resonator filter was built to verify the validity of the new method. The filter was tested over temperature with input circulators and output isolators to validate its suitability for practical applications such as satellite transponder input multiplexers.

The adaptive predistortion technique assumes no change to the filter topology and, thus, results in degraded return-loss performance. To compensate for the return-loss performance, these filters are connected with nonreciprocal devices such as isolators and circulators. Although it not a concern for satellite IMUX applications, it is always desirable to design filters with better return loss (RL) for those applications that do not allow the usage of ferrite devices. An alternative approach is to improve the response using lossy circuit techniques [5], [6], [9], [10]. These methods improve the RL using nonuniform dissipation and modified topologies with added loss. The use of resistive cross coupling and hyperbolic rotation was critical for the improvement of the filter response and the distribution of loss among the resonators. In this article, we will present physical insights for lossy filter design to create filters with finite-Q resonators and resistive couplings. A lossy four-pole microwave filter in mixed combline and microstrip technologies in the Ku band is designed, fabricated, and tested. Unlike the lossy realizations resulting from even and odd mode predistortion [9], all signal paths go through at least two resonators, eliminating unwanted source-to-load coupling especially at higher frequencies.

Adaptive Predistortion

In classic predistortion [8], the key step was to move the transmission poles (of the filter function) toward the $j\omega$ axis by a fixed amount denoted by r. To illustrate the use of this, let's examine the S-parameter

$$S_{21} = \frac{D(s)}{E(s)}, \tag{1}$$

where $s = j\omega$, ω is the angular frequency, $r = CF/(Q \times BW)$, CF is the center frequency, and BW is the bandwidth. The filter design process generally involves realizing the poles and zeros of the rational function: S_{21}. The transmission poles are the roots of polynomial $E(s)$ [1], while the transmission zeros are the roots of polynomial $D(s)$.

$$E(s) = c(s - p_1)(s - p_2)....(s - p_n), \tag{2}$$

where c is a constant and p_i is the ith root of $E(s)$.

When loss is modeled using the notion of dissipation factor r, $E(s)$ takes the form

$$E(s) = c\left[s - (p_1 - r)\right]....\left[s - (p_n - r)\right]. \tag{3}$$

The technique proposed in [3] introduced a constant shift of r in all the values p_i to combat the effect of dissipation factor in the transmission poles.

In contrast, the adaptive predistortion approach [3] is realized by introducing adaptive correction terms

$a_i (i = 1, 2, \ldots n)$ so that, including dissipation factor r, $E(s)$ takes the form

$$E(s) = c\left[s - (p_1 - r + a_1)\right] \ldots . \left[s - (p_n - r + a_n)\right]. \quad (4)$$

The adaptive correction terms a_i are arbitrary terms that can be virtually anything, as long as the law that governs physical realizability is not broken; i.e., keep all zeros of $E(s)$ in the left half of complex plane

$$\text{real}\left[p_i - r + a_i\right] < 0. \quad (5)$$

The correction terms a_i are then adjusted by an optimization algorithm to adapt the filter response into the required filter function. This process ensures that all a_i are changed at a different pace but adapts to the filter functions and specifications. The method in [8] then becomes a special case when all a_i are the same; i.e., $a_i = a$, where a is often called the predistortion term. If the desired Q value after predistortion is Q_p, then we obtain

$$a = \frac{CF}{BW}\left(\frac{1}{Q} - \frac{1}{Q_p}\right). \quad (6)$$

In general, a_i can be expressed using a as

$$a_i = v_i a, \quad (7)$$

where v_i is defined as the adaptive factor, or, in vector form, $\vec{v}$ and $v_i = 1$ is the special case for the method in [8]. The filter response S_{21}, also denoted herein as $F_a(s)$, can be calculated once again per (1) [3]. The filter response requirement (including shape and specifications) can be also defined as a function $R(s)$. An optimization method such as least square is then used to minimize

$$\min |F_a(s) - R(s)| \quad (8)$$

by adjusting a_i under the constraint of (5). A new set of roots of $E(s)$ is obtained as

$$t_i = p_i - a_i. \quad (9)$$

The final design filter function then takes the form of

$$S_{21}(s) = \frac{D(s)}{E'(s)}, \quad (10)$$

where

$$E'(s) = c(s - t_1)(s - t_2) \ldots . (s - t_n). \quad (11)$$

Note that through this process, no change has occurred in the transmission zeros [$D(s)$ in (1)].

High performance is defined as the most efficient use of the costly spectrum, which leads to a very flat filter passband and a steep transition into the rejection band while maintaining a small size and mass.

This adaptive predistortion technique will result in much less insertion loss, despite using low Q resonators, while other parameters such as loss variation will also be better than [7] and [8]. The small increase in group delay ripple (when using [8] for a self-equalized filter) can also be fixed adaptively. In one example, we analyzed a tenth-order filter typically used for satellite communications. The resonator used has a Q of 3,000. The target was to get equivalent performance of a filter with Q of 8,000. The adaptive vector is $\vec{v} = [0.7 \quad 1 \cdots 1 \quad 0.7]$. The first and last elements correspond to the poles near the $j\omega$ axis. The results are given in Table 1.

One may notice there is a 1.9-dB improvement in insertion loss and 1.6-dB improvement on RL. Although using any type of predistortion technique always leads to some level of insertion loss penalty, it is always very desirable to minimize the extra insertion loss. As can be seen from Table 1, using the technique in [2], [3] will lead to an additional 5.9-dB insertion loss in a low Q filter using predistortion. On the other hand, using the proposed method will result in only 4-dB added loss compared to a conventional dielectric resonator filter, which has an insertion loss of approximately 1.0 dB. This improvement is very significant as it could lead to a direct drop in type replacement of the current IMUX systems. The increase in LNA gain is within the range of adjustability of the amplifiers and may not require redesign to increase the gain (an extra stage).

In addition, the adaptive approach suggests that some of the elements of $\vec{v}$ can be greater than 1 while some of them are less than 1. That implies some of the poles can be overpredistorted while the poles near the $j\omega$ axis are underpredistorted to achieve the best overall results. This approach is necessary when much higher effective Q (same shape of S_{21} amplitude except absolute insertion loss) is required after predistortion. In the next section, we will demonstrate how this concept is applied to achieve a target Q of 20,000.

TABLE 1. Case study.

Parameters (dB)	Adaptive Predistortion	Predistortion [3]
Insertion loss	5.0	6.9
RL	3.6	2.0

Symmetrical Realization

The zeros of the reflection functions $S_{11}(s)$ and $S_{22}(s)$ of the predistorted filter characteristic in general will not be located on the imaginary axis [4]. For a synthesizable network, however, the zeros from $S_{11}(s)$ and $S_{22}(s)$ must form mirror-image pairs about the imaginary axis, to make it symmetric overall. Unlike the poles of the transfer and reflection function, there is no Hurwitz condition on the reflection zeros, and the individual zeros that make up the numerator polynomial of $S_{11}(s)$ may be arbitrarily chosen from the left-hand or right-hand side of each pair. $S_{22}(s)$ is made up from the remaining zeros from each pair to form the complementary function

$$S_{11} = \frac{F(s)}{E(s)} \quad S_{22} = \frac{F_{22}(s)}{E(s)}. \tag{12}$$

Thus, there are 2^N combinations of zeros that can be chosen to form $S_{11}(s)$ and $S_{22}(s)$, half of which are not simply exchanges; i.e., network reversals. Each different combination leads to different values for the coefficients of numerator polynomial and, after the synthesis process, different values for the network elements.

A parameter that may be used to broadly classify the solutions is μ, where

$$\mu = \left| \sum_{k=1}^{N} \mathrm{Re}(s_k) \right|$$

and s_k are the N zeros that have been chosen from the left-hand or right-hand sides of each pair to form $F(s)$. It may be demonstrated that if the zeros are chosen to minimize μ, then the values of the elements of the folded-array network will be maximally symmetric about the physical center of the network. However, the network will be tuned maximally asynchronous. The opposite also holds true: if μ is maximized, i.e., all the zeros for $F(s)$ are chosen from the left-hand or right-hand side of each mirror-image pair, now the network will be close to being synchronously tuned. However, this time, the network elements values will be maximally asymmetric about the center of the network. Figure 3 shows a few possible arrangements for the zeros $F(s)$.

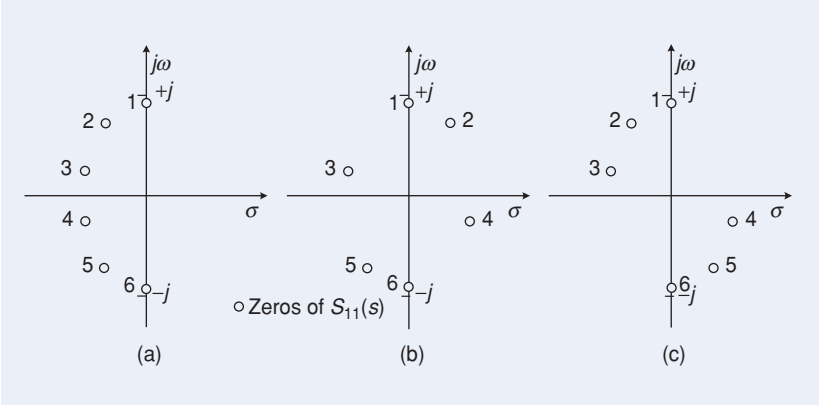

Figure 3. *Possible arrangements for the zeros s_k of $F(s)$ for the symmetric 6-2 quasi-elliptic characteristic. (a) μ = max. (b) μ = 0. (c) μ = 0.*

Lossy Circuit Techniques

Lossy circuit techniques [5], [6], [9] use nonuniform dissipation and modified topologies with extra lossy coupling elements to realize a low Q filter with high flatness and good RL. In [9], a generalized coupling matrix synthesis approach was presented. However, to illustrate the idea of lossy circuit realization in a simplistic fashion, an alternative but more limited representation is presented here. The intent is to provide readers with more physical insights of lossy filter techniques. Consider the general

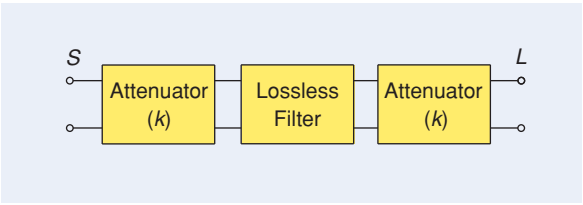

Figure 4. *A possible representation of a lossy filter with RL and insertion loss shifted down.*

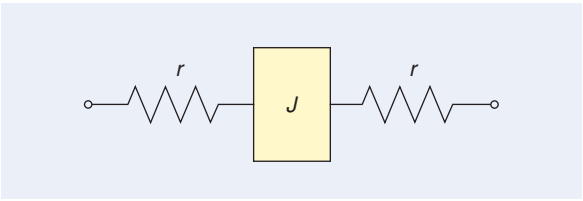

Figure 5. *Attenuator model with a J-inverter and two identical resistors.*

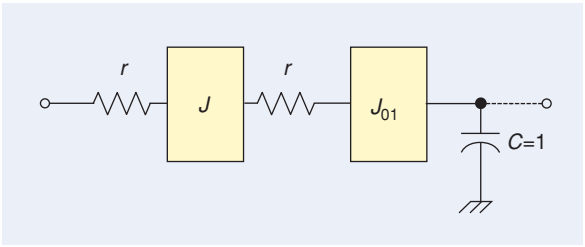

Figure 6. *First/last resonator connected to an attenuator.*

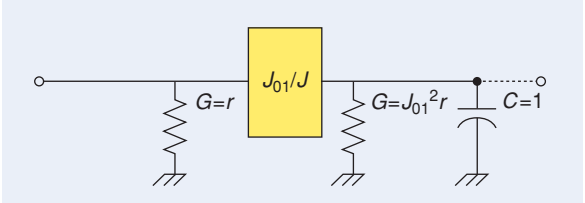

Figure 7. *Equivalent circuit of Figure 6.*

diagram for a lossless filter with two matched attenuators at source and load as in Figure 4.

Since the attenuators are matched at both ports, the overall lossy scattering parameters in terms of the lossless ones become

$$\begin{aligned} S_{11}^{\text{lossy}} &= k^2 S_{11} \\ S_{22}^{\text{lossy}} &= k^2 S_{22} \\ S_{21}^{\text{lossy}} &= k^2 S_{21}, \end{aligned} \tag{13}$$

where k is the amount of attenuation. One way to realize an attenuator is using a J-inverter with resistors as shown in Figure 5.

The following relationships apply for this attenuator model as follows:

$$J = \pm \frac{1}{\sqrt{1-r^2}}, \quad k = \sqrt{\frac{1-r}{1+r}}. \tag{14}$$

Assume that the attenuators described in the previous section are connected to the first (last) resonator of a filter as shown in Figure 6. For simplicity, only the first resonator is shown for an arbitrary order filter.

By moving the two resistors to the right-hand side of the inverters, proper scaling can be used to scale the first inverter to unity and thus can be removed as it acts as a 90° transmission line. The final circuit is shown in Figure 7.

By placing an identical attenuator at the output port, simple synthesis for the coupling matrix can be obtained. The realization is limited to the case with loss appearing only at the first and last resonators along with shunt resistors at input and output ports. It does not apply to transversal filters either.

The original lossless $N+2$ coupling matrix (nontransversal) can be presented as in Figure 8. The lossy coupling matrix in terms of the lossless coupling matrix is shown in Figure 9 considering the changes at the input/output port. The new parameters in the lossy coupling matrix have the following relation to the lossless coupling elements, which make the lossy synthesis formulas

$$\begin{aligned} G'_S &= G'_L = r = \frac{1-k^2}{1+k^2}, \\ J'_{S1} &= \pm J_{S1}\sqrt{1-r^2}, \quad J'_{NL} = \pm J_{NL}\sqrt{1-r^2} \\ G'_1 &= J_{S1}^2 r, \quad G'_N = J_{NL}^2 r. \end{aligned} \tag{15}$$

As it is clear from these equations, the maximum loss absorbed in the resonator is when the maximum loss is applied to the circuit; i.e., $k = 0$ or $r = 1$. In this case the minimum normalized Q that can be absorbed to the first/last resonator is

$$Q_{1\_\min} = \frac{1}{J_{S1}^2}, \quad Q_{N\_\min} = \frac{1}{J_{NL}^2}. \tag{16}$$

This type of synthesis is very easy and convenient, especially for cases where hyperbolic rotation [5] is used to distribute the loss among the resonators. The lossy coupling matrix in this format can be derived easily from a synthesized lossless coupling matrix.

	S	1	2	…	$N-1$	N	L
S	0	J_{S1}	0	…	0	0	0
1	J_{S1}	J_{11}	J_{12}	…	$J_{1,N-1}$	J_{1N}	0
2	0	J_{12}	J_{22}	…	$J_{2,N-1}$	J_{2N}	0
⋮	⋮	⋮	⋮	⋱	⋮	⋮	⋮
$N-1$	0	$J_{1,N-1}$	$J_{2,N-1}$	…	$J_{N-1,N-1}$	$J_{N-1,N}$	0
N	0	J_{1N}	J_{2N}	…	$J_{N-1,N}$	J_{NN}	J_{NL}
L	0	0	0	…	0	J_{NL}	0

Figure 8. *Lossless $N+2$ coupling matrix.*

	S	1	2	…	$N-1$	N	L
S	$-jG'_S$	J'_{S1}	0	…	0	0	0
1	J'_{S1}	$J_{11}-jG'_1$	J_{12}	…	$J_{1,N-1}$	J_{1N}	0
2	0	J_{12}	J_{22}	…	$J_{2,N-1}$	J_{2N}	0
⋮	⋮	⋮	⋮	⋱	⋮	⋮	⋮
$N-1$	0	$J_{1,N-1}$	$J_{2,N-1}$	…	$J_{N-1,N-1}$	$J_{N-1,N}$	0
N	0	J_{1N}	J_{2N}	…	$J_{N-1,N}$	$J_{NN}-jG'_N$	J'_{NL}
L	0	0	0	…	0	J'_{NL}	$-jG'_L$

Figure 9. *Lossy $N+2$ coupling matrix.*

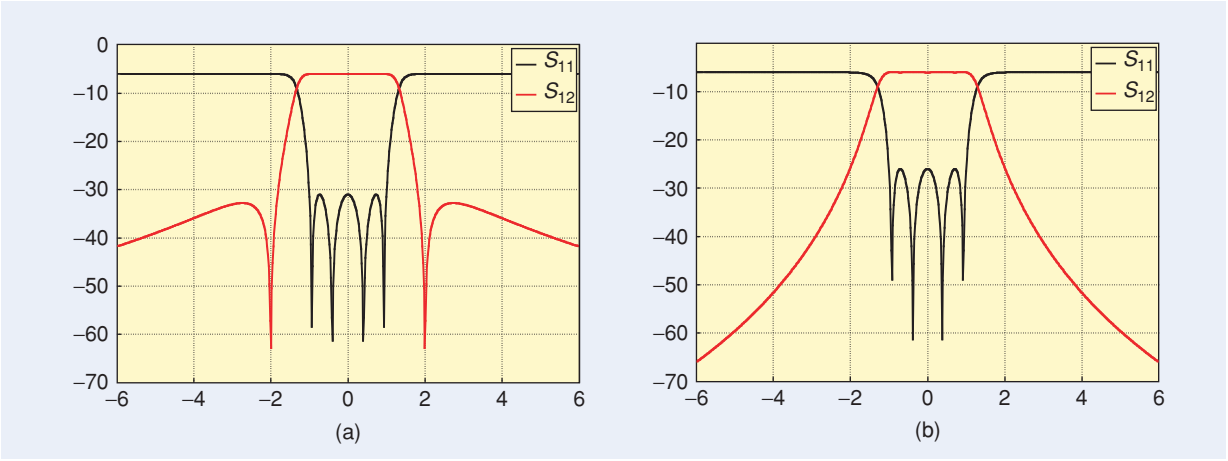

Figure 10. *Four-pole lossy examples (from [9]).*

Four-Pole Chebyshev Examples

We consider here four-pole Chebyshev and quasi-elliptic examples [9]. Consider the two filter responses shown in Figure 10. Both responses are down 6 dB compared to their lossless equivalent.

In order to synthesize the coupling matrix for these two filters, first the lossless $N+2$ coupling matrices of the two filters need to be synthesized. The two matrices are shown in Figures 11 and 12.

Using the synthesis equations in the previous section with a 6-dB loss (i.e., 3-dB attenuators at both sides, $k = 0.7079$), the attenuator parameter r is calculated as

$$r = \frac{1-k^2}{1+k^2} = 0.3323. \tag{17}$$

Using the r value in (15), the final $N+2$ lossy matrices can be calculated as shown in Figures 13 and 14.

The two synthesized coupling matrices match with the ones reported in [9], which verifies the validity of this approach. This matrix can be used as a starting point for further rotations to obtain other desired solutions. One desired realization is to have the loss equally distributed among the resonators. This can be done using hyperbolic rotations [5]. The final coupling matrix for the Chebyshev example has been calculated using hyperbolic rotations and proper node scaling [9] as shown in Figure 15. This matrix is obtained by hyperbolic rotations of $-6.21°$ on pivot [1 2], $6.21°$ on pivot [3 4], and scaling the source and load nodes by a factor of 0.319.

The node diagram of this filter is shown in Figure 16, where the black circles represent resonators and empty circles are nonresonating nodes.

	S	1	2	3	4	L
S	0	1.035	0	0	0	0
1	1.035	0	0.911	0	0	0
2	0	0.911	0	0.7	0	0
3	0	0	0.7	0	0.911	0
4	0	0	0	0.911	0	1.035
L	0	0	0	0	1.035	0

Figure 11. *The lossless coupling matrix for the four-pole Chebyshev filter with return loss(RL) of 20 dB.*

	S	1	2	3	4	L
S	0	1.134	0	0	0	0
1	1.134	0	0.974	0	–0.248	0
2	0	0.974	0	0.854	0	0
3	0	0	0.854	0	0.974	0
4	0	–0.248	0	0.974	0	1.134
L	0	0	0	0	1.134	0

Figure 12. *Lossless coupling matrix for the four-pole filter with transmission zeros at $\pm j2$ and RL = 25 dB.*

	S	1	2	3	4	L
S	–j0.332	0.9762	0	0	0	0
1	0.9762	–j0.356	0.911	0	0	0
2	0	0.911	0	0.7	0	0
3	0	0	0.7	0	0.911	0
4	0	0	0	0.911	–j0.356	0.9762
L	0	0	0	0	0.9762	–j0.332

Figure 13. *Lossy coupling matrix for the four-pole Chebyshev filter.*

	S	1	2	3	4	L
S	–j0.332	1.0696	0	0	0	0
1	1.0696	–j0.427	0.974	0	–0.248	0
2	0	0.974	0	0.854	0	0
3	0	0	0.854	0	0.974	0
4	0	–0.248	0	0.974	–j0.427	1.0696
L	0	0	0	0	1.0696	–j0.332

Figure 14. *Lossy coupling matrix for the four-pole filter with a pair of transmission zeros.*

Lossy Resonator Q Limitation

In this section, we try to illustrate the limitation of lossy resonators in respect to the minimum loss that can be accepted without affecting the equivalent lossless performance. Consider a resonator with a normalized Q of Q_0 to make a one-pole filter, as shown in Figure 17. This one-pole filter can be thought of as a fundamental building block in a general microwave filter and can be used to calculate the loss limitation of the particular resonator.

The conductor representing the resonator loss can be split into two conductors, G_1 and G_2, and transferred as series resistors at the other sides of the two J-inverters as in Figure 18.

The middle network in Figure 18 is the original lossless ideal one-pole filter. Now using the diagram in Figure 4, the two resistors can be absorbed in two attenuators with the configuration shown in Figure 5. The two attenuation sections are then easily designed by the following:

$$r_1 = G_1/J_1^2, \quad r_2 = G_2/J_2^2,$$
$$k_1 = \sqrt{\frac{J_1^2 - G_1}{J_1^2 + G_1}}, \quad k_2 = \sqrt{\frac{J_2^2 - G_2}{J_2^2 + G_2}}, \tag{18}$$

where k_1 and k_2 are attenuation factors at the left and right, respectively.

The quality factor of the resonator can then be calculated as

$$Q = \frac{1}{G} = \frac{1}{G_1 + G_2} = \frac{1}{r_1 J_1^2 + r_2 J_2^2}. \tag{19}$$

From (14), it is clear that the series resistor cannot be greater than one. This gives us a good measure to find the minimum possible Q as

$$Q_{\min} = \frac{1}{J_1^2 + J_2^2}. \tag{20}$$

To get a practical sense of this limit, let's assume that the two J-inverters have unity value. Then the minimum normalized Q becomes $Q_{\min} = 0.5$. This one-pole lossy filter design is a very good example to understand the limitations of the lossy filter synthesis, as it can be considered a fundamental building block of a lossy resonator in the overall filter. It can also be considered as the best possible scenario to absorb maximum loss. When more lossless resonators are present, the loss distribution will cause less average loss for each resonator and thus higher Q values.

Realization of Adaptive Predistortion at the C Band

One of the main objectives for developing the predistorted filter is to reduce the mass and volume over the current C-band single-mode dielectric resonator technology used. The standard coaxial cavity resonator was selected for its simplicity, excellent Q-to-volume ratio given its compact size,

	S	1	2	3	4	L
S	–j0.339	0.3137	j0.0339	0	0	0
1	0.3137	–j0.1611	0.8932	j0.0765	–0.0083	0
2	j0.0339	0.8932	–j0.1949	0.7082	j0.0765	0
3	0	j0.0765	0.7082	–j0.1949	0.8932	j0.0339
4	0	–0.0083	j0.0765	0.8932	–j0.1611	0.3137
L	0	0	0	j0.0339	0.3137	–j0.0339

Figure 15. *Coupling matrix with equal Q values. The input/output coupling values are 0.319.*

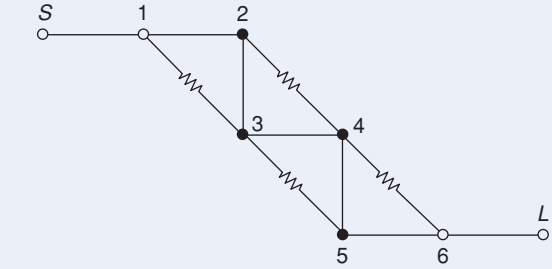

Figure 16. *The node diagram of the four-pole filter.*

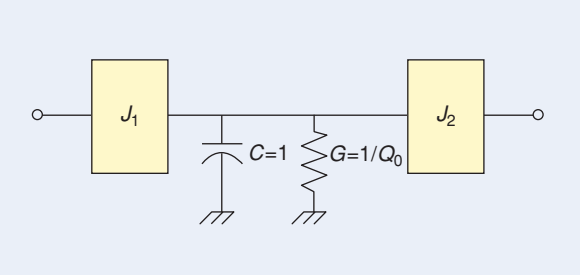

Figure 17. *A single-pole filter model.*

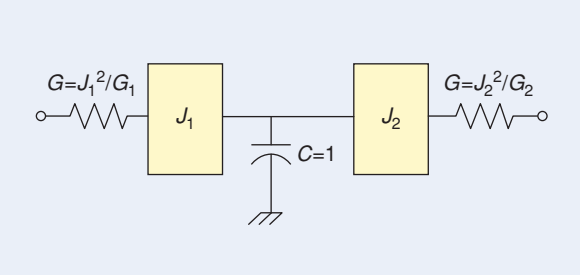

Figure 18. *Equivalent circuit with loss transferred out of the resonator.*

simple temperature compensation leading to excellent temperature stability, and ability to be readily qualified due to its similarity with past coaxial flight hardware. Using a typical C-band filter of 1% bandwidth and a ten-pole self-equalized transfer function design, a series of simulations were performed to determine the optimal trade-off between cavity size and insertion loss with a targeted equivalent Q of 20,000. Equivalent (or effective) Q is used here to define the filter transmission shape, except absolute insertion loss, that is comparable to a filter implemented at that $Q3$ level. The result of the trade-off is shown in Table 2.

To create a 10-4-4 filter using the procedure given in the last sections, the following eight transmission zeros are chosen (RL level set at 22 dB):

$$\pm 1.09912\,j$$
$$\pm 1.605389\,j$$
$$\pm 0.61730 \pm 0.34881\,j.$$

Following the process defined previously, a solution of $\vec{v} = [0.4 \quad 1.5 \quad \cdots \quad 1.5 \quad 0.4]$ is selected. That means the poles near the $j\omega$ axis are moved (underpredistorted) 0.4 times less than the standard predistortion [3] and all other poles are moved 1.5 times more (overpredistorted). The adaptively predistorted poles now sit at

$$-0.020300 \pm 1.030902\,j$$
$$-0.097168 \pm 0.972767\,j$$
$$-0.225218 \pm 0.750657\,j$$
$$-0.252744 \pm 0.445003\,j$$
$$-0.263617 \pm 0.155519\,j.$$

The coupling matrix derived through this process is

$$M_{11} = M_{22} = M_{33} = M_{44} = M_{55} = M_{66} = M_{77} = M_{88} = M_{99} = M_{10,10} = 0$$
$$M_{12} = 0.70514,\ M_{23} = 0.54767,\ M_{34} = 0.49894,\ M_{45} = 0.49391,$$
$$M_{56} = 0.62432,\ M_{67} = 0.53824,\ M_{78} = 0.56020,\ M_{89} = 0.64935,$$
$$M_{9,10} = 1.07017,\ R_1 = 0.1307,\ R_{10} = 1.5800$$
$$M_{1,10} = 0.01434,\ M_{29} = -0.01999,\ M_{38} = -0.08992,\ M_{47} = -0.00369.$$

It is also interesting to point out that he reflection zeros (S_{11}) will no longer be on the $j\omega$ axis :

$$-0.000000 \pm 1.018419\text{j}$$
$$-0.071729 \pm 0.967019\text{j}$$
$$-0.197336 \pm 0.745597\text{j}$$
$$-0.222897 \pm 0.443401\text{j}$$
$$-0.232933 \pm 0.154880\text{j}.$$

A low-cost coaxial resonator structure (combline) using 0.5 × 0.5 × 0.7-in cavities was selected to construct the low Q ($Q = 3,000$) filter, resulting in an overall filter dimension of 1.1 × 3.0 × 0.9 in for a ten-pole design. The length of the post inside a cavity is about 0.6 in, which leaves a gap of 0.1 in. The filter housing is largely fabricated using aluminum for low mass. Invar is used for the coaxial posts (0.3 in) for temperature compensation. The filter is shown in a side-by-side comparison to a typical dielectric resonator filter in Figure 19. The center frequency is 3.952 GHz and bandwidth is approximately 39 MHz. The larger filter with a Q of 8,000 represents current technology being used for input multiplexers in satellite transponders. Both filters are of the same frequency and order. The volume of the smaller coaxial filter is approximately 25% of the larger dielectric filter with a mass of approximately 35% that of the larger; net reductions of 75% and 65%, respectively. The predistorted filter is designed to have an equivalent Q of 20,000 with an insertion loss of 5.7 dB. The size of the filter is almost comparable to the typical Ku-band dielectric IMUX filter as shown in the next section.

TABLE 2. Insertion loss versus intrinsic Q for an equivalent Q of 20,000.

		Insertion Loss (dB)	
		Before	After
Intrinsic Q	Cavity Size (Inches)	Predistortion	
1,000	0.15 × 0.15 × 0.8	7.7	24.7
2,000	0.3 × 0.3 × 0.75	3.9	10.4
3,000	**0.5 × 0.5 × 0.7**	**2.6**	**5.7**
4,000	0.7 ×0.7 × 0.62	1.9	3.9
5,000	1.0 ×1.0 × 0.5	1.6	2.9

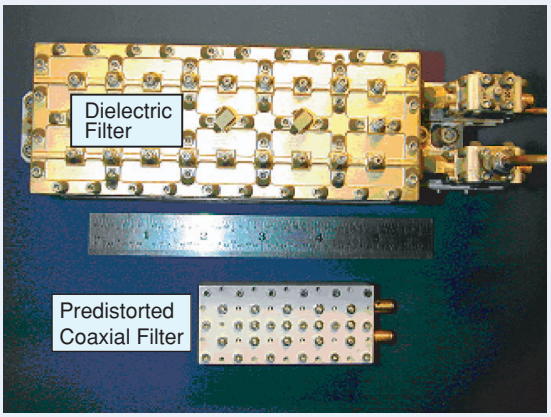

Figure 19. *A coaxial resonator predistorted filter and a conventional dielectric resonator filter.*

The measured performance of the adaptively predistorted filter is shown in Figure 20(a)–(c). Both transmission and loss variation plots in Figure 3(a) and (b) are normalized to 5.9dB (which is the measured insertion loss, compared to a designed value of 5.7 dB). The in-band insertion loss variation is less than 0.1 dB and the in-band group delay is less than 2 ns. To estimate the equivalent Q, the measured loss variation is compared to the computer-simulated performance of filters with ideal Q, and the comparison is presented in Figure 21. From this comparison, the equivalent Q of the measured filter is estimated to be above 20,000. This set of measured data clearly confirms that by implementing the adaptive predistortion technique the performance of a low Q coaxial filter as a minimum is comparable (group delay) to or significantly better (loss variation) than that of a high Q dielectric filter. A much higher equivalent Q can be easily realized using this approach. The method can also be applied to high Q filters, although the advantage would be less impressive. The designed filter was also tested for stability and drift over temperature. Less than 0.5 ppm frequency drift was observed over a 40 °C span.

Filter Realization at the Ku Band

Asymmetric Realization

Ku-band IMUX filters often have similar bandwidth to their C-band counterparts, which means that the proportional bandwidth is about three times narrower compared to the C-band. In order to achieve comparable predistortion results at the Ku band, the starting Q for Ku-band resonators needs to be

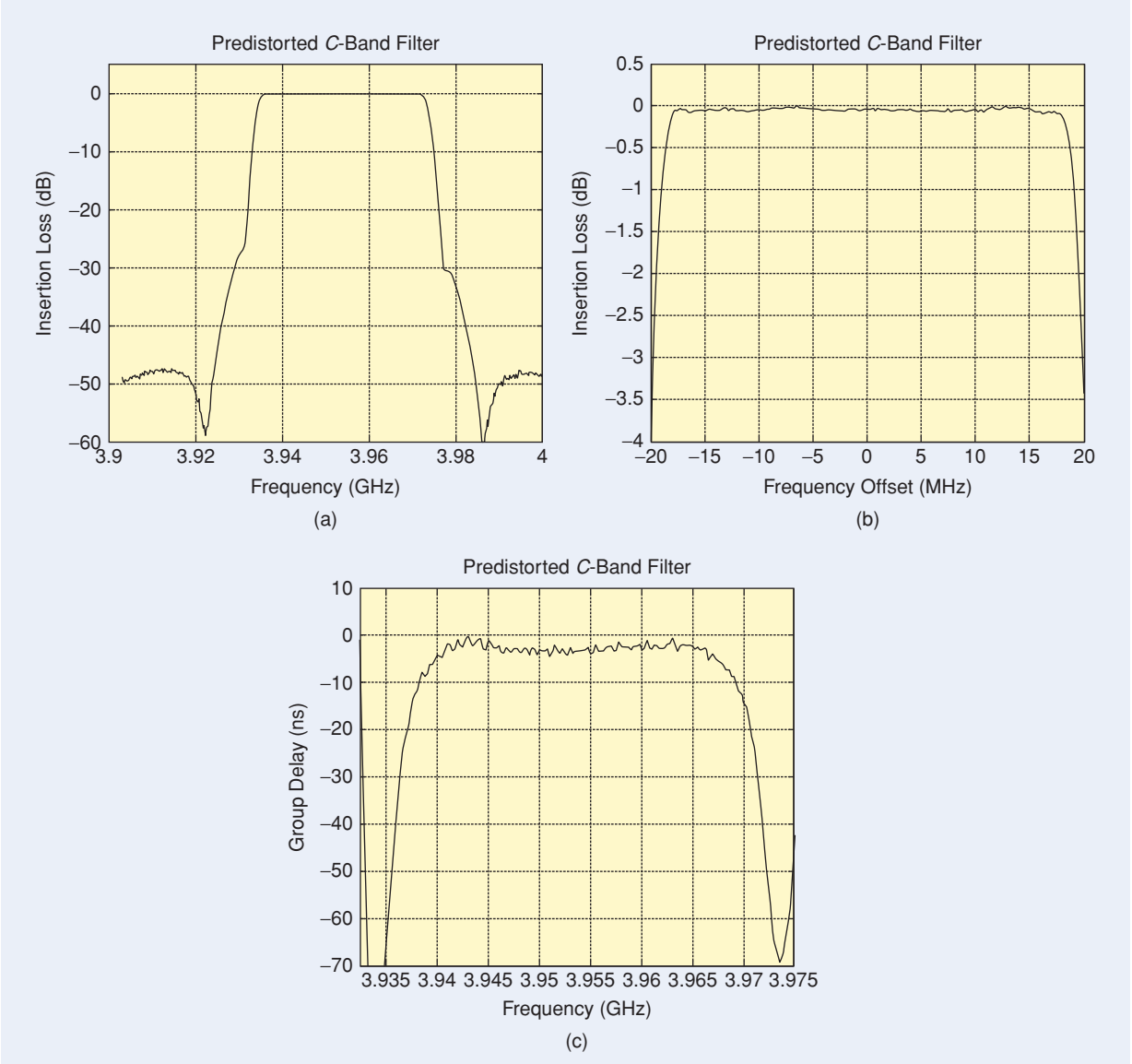

Figure 20. *(a) Measured transmission (S_{21}) performance (normalized to 5.9 dB). (b) Measured in-band loss (S_{21}) variation performance. (c) Measured group delay performance.*

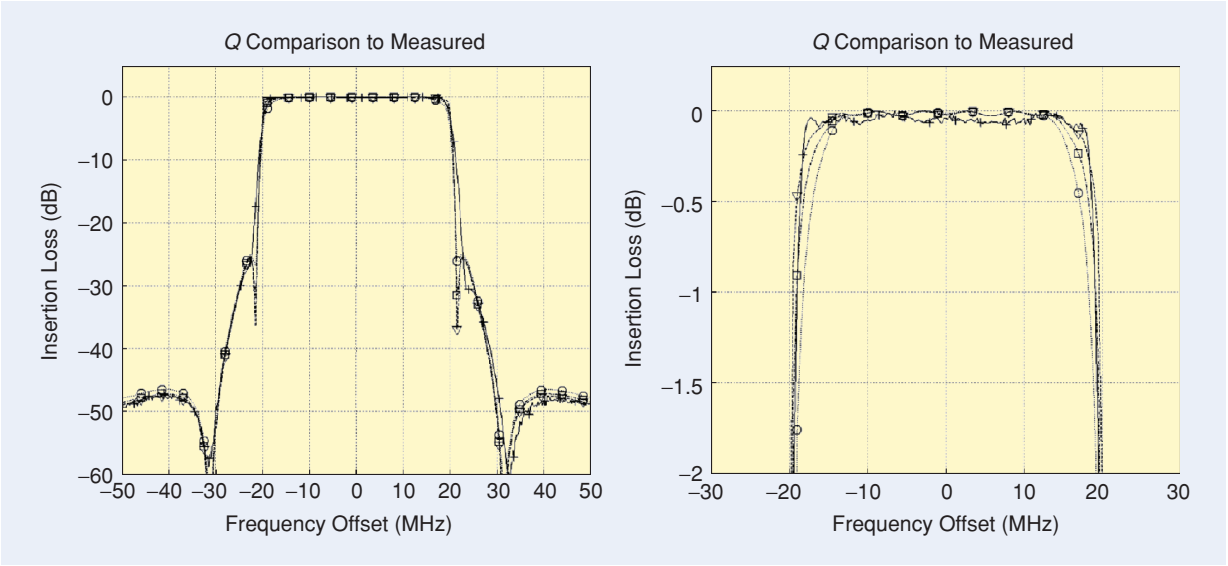

Figure 21. *Measured loss (normalized to 5.9 dB) versus simulated with ideal Q (also normalized).*

around 9,000. This limitation pretty much rules out the possibilities of using inexpensive coaxial filter technology to replace current dielectric technology. On the other hand, the much improved in-band performance achievable with adaptively predistorted filters still justifies the development of a Ku-band version using dielectric resonator technology. In addition, we will also show that other bandwidth enhancement features can also be achieved by extending the adaptive approach. This will become more obvious in the next section.

Dielectric loaded resonators ($Q = 8,000$) using $0.4 \times 0.4 \times 0.35$-in cavities were selected to construct the Ku-band filter. The 10-4-4 filter using $TE_{01\delta}$ mode is shown in Figure 22. There are no structural differences in comparison with the commonly used Ku-band IMUX filter, except for the internal iris/probe sizes. The center frequency is 12.65 GHz and bandwidth is approximately 50 MHz. The (preliminary) measured performance of the adaptively predistorted filter is shown in Figure 23(a)–(c) and is consistent with an equivalent Q of 20,000. The research is still going on and more results will be reported later.

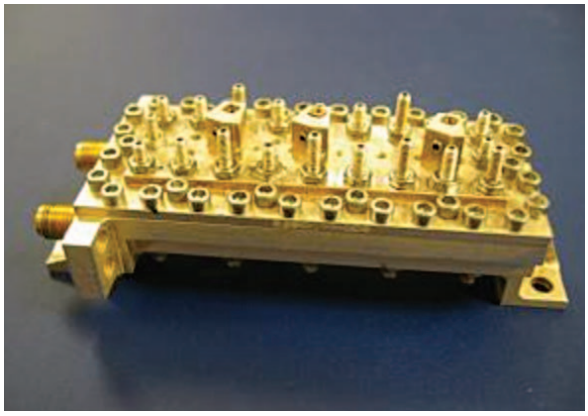

Figure 22. *A predistorted dielectric resonator filter at the Ku-band.*

Symmetric Realization

In a similar way to asymmetric realization, dielectric loaded resonators using $TE_{01\delta}$ mode ($Q = 8,000$) and $0.4 \times 0.4 \times 0.35$-in cavities were selected to construct the Ku-band filter. Following the theory given in the last section, the coupling matrix for a 10-4-4 filter case is derived for a target Q of 15,000:

$$M_{11} = -M_{10,10} = -0.04498, M_{22} = -M_{99} = 0.00761$$
$$M_{33} = -M_{88} = 0.06255, M_{44} = -M_{77} = -0.01931$$
$$M_{55} = -M_{66} = -0.20402, R_1 = R_{10} = 0.80005$$
$$M_{12} = M_{9,10} = 0.74118, M_{23} = M_{89} = 0.57447$$
$$M_{34} = M_{78} = 0.55131, M_{45} = M_{67} = 0.52636,$$
$$M_{56} = 0.38676,$$
$$M_{1,10} = 0.00355, M_{29} = -0.01875, M_{38} = -0.0260,$$
$$M_{47} = 0.13376,$$

where the transmission zeros are (RL level set at 22 dB) at

$$\pm 1.27359j$$
$$\pm 1.93825j$$
$$\pm 0.58087 \pm 0.33908j.$$

The 10-4-4 filter exhibits no structural differences from the commonly used Ku-band IMUX filter except that the fifth and sixth resonators are tuned to a different center frequency from the rest. This feature enables the design of a regular (nonpredistorted) filter, followed by custom tuning of the resonators to achieve the required

performance enhancement by varying the predistortion (different equivalent Q level). All physical dimensions such as iris size and probe length remain very close to the original Chebyshev filter.

A 10-4-4 IMUX filter with input circulators and output isolators was built and tested over a 60 °C temperature range. The IMUX filter is often tuned to match the input circulator and output isolator. Center frequency is 12.467 GHz and bandwidth is 31 MHz.

All insertion loss measurements were done at hot (62 °C), cold (2 °C), and ambient (23 °C) for easy comparison. Figure 24(a) shows the insertion loss measurements at cold, hot, and ambient temperatures using two different frequency scales. The data clearly show that there are very minimal changes in isolation. Figure 24(b) gives a magnified view of Figure 24(a) over the filter passband. Less than 0.1-dB ripple was observed. Figure 24(c) shows the in-band group delay and its stability data at the same temperature range. The presented data clearly confirm that 1) symmetrical realization of predistorted filters can achieve superior in-band performance and 2) even with input circulator and output isolators, no undesirable insertion loss ripple was observed over temperature. The insertion loss ripple caused by multipath effects (partially addressed in [3]) is not of concern for predistorted filters as it is observed from the presented test data.

The coupling matrix is extracted as

$$
\begin{aligned}
&M_{11} = -0.0397,\ M_{10,10} = -0.0691,\\
&\quad M_{22} = -0.0036,\ M_{99} = -0.0067\\
&M_{33} = 0.0075,\ M_{88} = -0.0113,\\
&\quad M_{44} = -0.0174,\ M_{77} = 0.0044\\
&M_{55} = -0.1986,\ M_{66} = 0.1971,\\
&\quad R_1 = 1.0541,\ R_{10} = 1.0326\\
&M_{12} = 0.8273,\ M_{9,10} = 0.8318,\\
&\quad M_{23} = 0.5832,\ M_{89} = 0.5817\\
&M_{34} = 0.5460,\ M_{78} = 0.5454,\\
&\quad M_{45} = 0.5244,\ M_{67} = 0.5226\\
&M_{56} = 0.5048,\ M_{1,10} = 0.005,\\
&\quad M_{29} = -0.05,\ M_{38} = -0.005\\
&M_{47} = 0.05.
\end{aligned}
$$

Of course, in a practical realization, it is expected that a slightly asymmetric distribution of the coupling values will occur

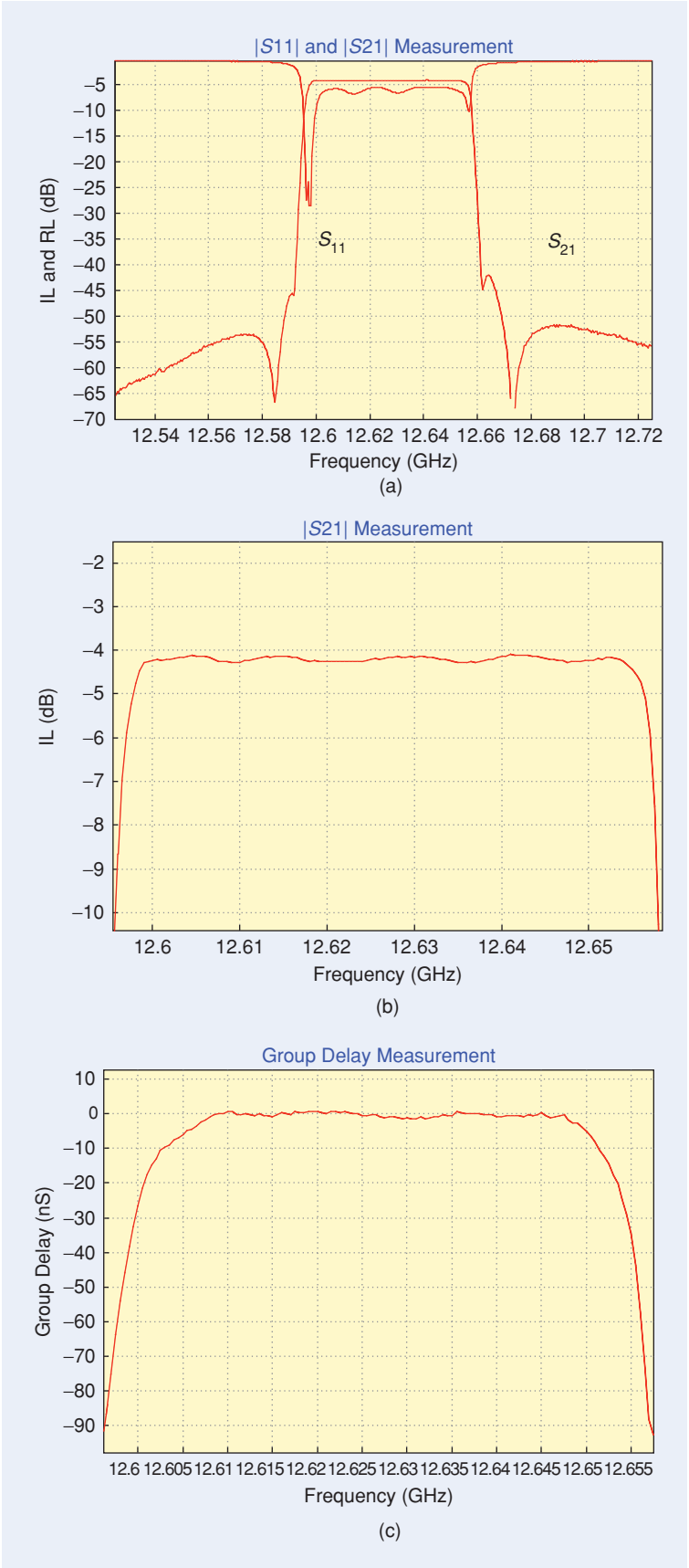

Figure 23. *(a) Measured RL (S_{11}) and insertion loss (S_{21}) performance. (b) Measured loss variation performance (not normalized). (c) Measured group delay performance.*

since the filter is manually tuned with the aid of computer software.

Lossy Filter Realization

To validate the lossy synthesis technique, we considered the design of a four-pole Chebyshev filter with mixed microstrip and combline technologies, with resonators in combline and the resistive sections in microstrip technology [9], [10]. To create a coupling matrix for resonators with a Q of approximately 2,000 and a fractional bandwidth of 1%, the loss level needs to be changed to −2.9 dB. The lossless RL is chosen to be 25 dB. The new synthesized coupling matrix with equally distributed loss is shown in Figure 25.

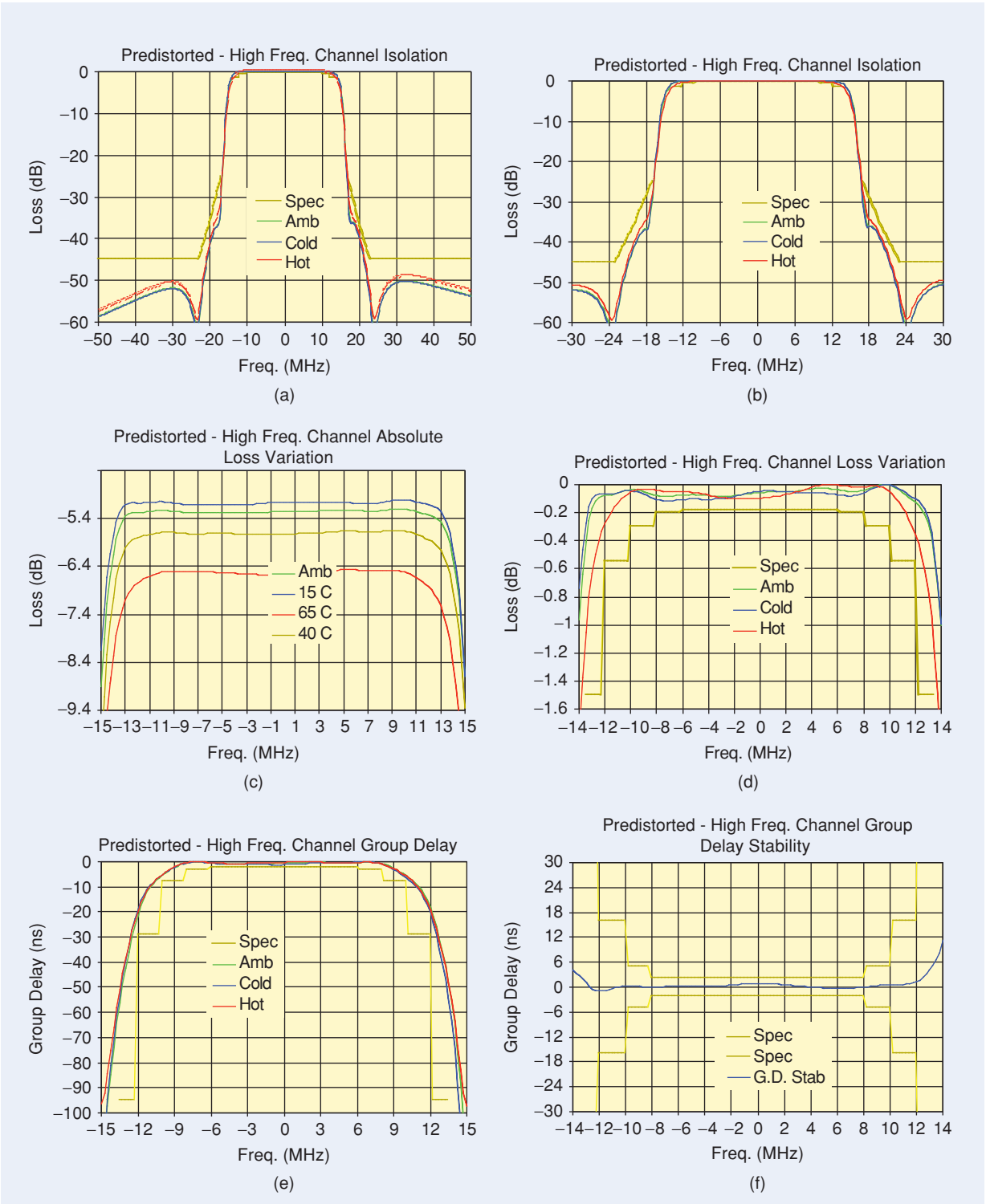

Figure 24. *Measured 10-4-4 filter data.*

The resistive cross-coupling elements are designed using microstrip technology with chip resistors, while the resonators are designed using combline technology, which has a better quality factor compared to microstrip. The complete filter was modeled as shown in Figure 26. The picture of the fabricated filter next to a quarter coin is shown in Figure 27(a). Figure 27(b) shows the packaged four-pole lossy filter next to two other filters in the Ku band: a dielectric four-pole filter ($TE_{01\delta}$ mode) and a four-pole dual mode cavity filter (TE_{113} mode). The size of the manufactured lossy filter appears to be approximately the same as the dielectric one, because the current lossy layout design is far from optimum. The dielectric filters have a cross-section dimension of 12.7 mm^2 ($0.5 \times 0.5\,in.^2$), while the lossy filter cavities have a size of 6.35 mm^2 ($0.25 \times 0.25\,in.^2$). This indicates that the lossy filter size can be reduced by a factor of four by mounting the microstrip circuits from the bottom of the cavities [10].

The measured filter response is shown in Figure 28. The measured passband ripple is approximately 0.5 dB due to a lower actual Q of about 1,300 compared to 2,000. The equivalent Q obtained is about 3,500. In order to compensate for the discrepancy between the actual Q and the one used for synthesis, a new synthesis for the actual Q of 1,300 is needed, which results in different resistor and coupling values. Since the chip resistors are not tunable, the ripple cannot be further improved. However, using a tunable resistor will solve this problem.

Figure 28 also shows the synthesized response with a bandwidth of 124 MHz and the extracted response using optimization. As seen from the response, the measured rejection in the lower frequency band has degraded, while the rejection in the upper frequency band has

	S	1	2	3	4	L
S	$-j0.0278$	0.4667	$j0.0278$	0	0	0
1	0.4667	$-j0.0959$	1.0352	$j0.0461$	-0.0027	0
2	$j0.0278$	1.0352	$-j0.1237$	0.7743	$j0.0461$	0
3	0	$j0.0461$	0.7743	$-j0.1237$	1.0352	$j0.0278$
4	0	-0.0027	$j0.0461$	1.0352	$-j0.0959$	0.4667
L	0	0	0	$j0.0278$	0.4667	$-j0.0278$

Figure 25. *Coupling matrix with fabrication for Q of 2,000. The input/output coupling values are 0.41.*

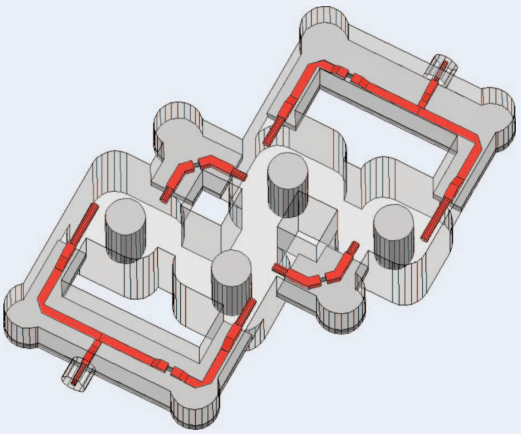

Figure 26. *The three-dimensional (3-D) model of the complete lossy filter.*

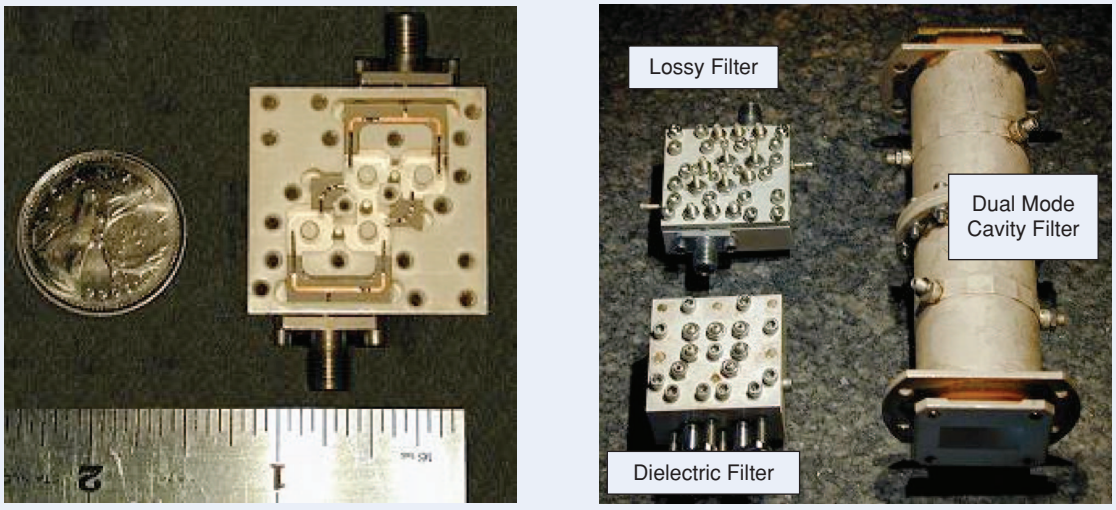

Figure 27. *Picture of the fabricated lossy filter using mixed technologies. (a) The filter structure. (b) The packaged filter next to the four-pole dielectric ($TE_{01\delta}$ mode) and dual mode cavity (TE_{113} mode) filters.*

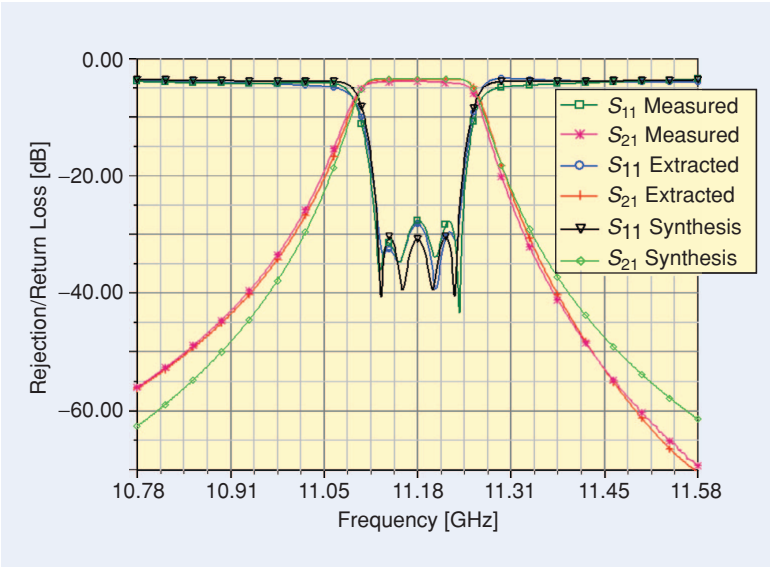

Figure 28. *Measurement versus synthesis and extracted results at 11.18 GHz.*

improved compared to the synthesis. From circuit extraction, it becomes apparent that this is due to unwanted 1–3 and 2–4 small coupling values ($m_{13} = m_{24} = 0.045$).

The reason for choosing a lower-order filter compared to predistortion is to prove the concept and to overcome the realization issues. The lossy approach is still at its early stages of development and needs more research and development effort to become as mature as the predistorted filters.

Conclusions

An adaptive predistortion technique has been presented and verified through the design and fabrication of practical filters in both the C and Ku bands. The method allows the realization of microwave filters at a lower cost, lighter mass, smaller volume, and better performance with minimum insertion loss penalties.

The main penalty in using predistortion is in the increase of absolute insertion loss; however, the increase caused by the adaptive technique is significantly less than the previously reported classical predistortion technique. Typically, with an adaptive algorithm, an additional loss of as much as 4–5 dB will be incurred over the conventional high Q filters currently used. However, since the targeted application is for those filters located after the LNA/receiver circuit (or after one low-gain LNA), one should be able to increase the gain of the later stages to compensate for the increase in loss without impacting the noise figure of the system.

The perceived tuning issue from the past can be solved using well-established computer-aided tuning techniques. The excellent performance achieved in this article proves that this technique is ready for practical applications.

The concept of lossy filters has been presented from a practical perspective. A simple lossy synthesis technique using any synthesized lossless (nontransversal) filter was shown, which can be used with hyperbolic rotations for loss distribution. Moreover, the limitation on the minimum Q of lossy resonators has been studied using a one-pole filter as a fundamental building block. Lossy four-pole Chebyshev and quasi-elliptic synthesis examples were presented. A four-pole Chebyshev lossy filter in the Ku band has been synthesized, modeled, and fabricated successfully using mixed combline and microstrip technologies. The design has the advantage of having all input–output paths going through more than one resonator, which minimizes unwanted source-to-load coupling, especially at high frequencies. The lossy approach is still at its early stages of development and needs more research and development effort to become as mature as the predistorted filters.

The presented techniques should lead to significant improvement for applications such as satellite transponder input multiplexers, wireless ground base stations, repeaters, and wherever insertion loss can be traded off for in-band flatness, mass, volume, and overall system performance.

References

[1] R.J. Cameron, C. Kudsia, and R. Mansour, *Microwave Filters for Communication Systems*. Hoboken, NJ: Wiley, 2007.

[2] A.C. Guyette, I.C. Hunter, and R.D. Pollard, "A new class of selective filters using low-Q components suitable for MMIC implementation," in *IEEE MTT-S Int. Microwave Symp. Dig.*, 2004, vol. 3, pp. 1959–1962.

[3] M. Yu, W.-C. Tang, A. Malarky, V. Dokas, R. Cameron, and Y. Wang, "Novel adaptive predistortion technique for cross coupled filters and its application to satellite communication systems," *IEEE Trans. Microwave Theory Tech.*, vol. 51, no. 12, pp. 2505–2514, Dec. 2003.

[4] M. Yu, R. Cameron, D. Smith, V. Dokas, and Y. Wang, "Symmetrical realization for predistorted microwave filters," in *IEEE MTT-S Int. Microwave Symp. Dig.*, Long Beach, CA, June, 2005, pp.245–248.

[5] A. Guyette, I. Hunter, and R. Pollard, "The design of microwave bandpass filters using resonators with nonuniform Q," *IEEE Trans. Microwave Theory Tech.*, vol. 54, no. 11, pp. 3914–3922, Nov. 2006.

[6] A. Guyette, I. Hunter, and R. Pollard, "Exact synthesis of microwave filters with nonuniform dissipation," in *Proc. IEEE MTT-S Int. Microwave Symp.*, Honolulu, HI, June 2007, pp. 537–540.

[7] R.M. Livingston, "Predistorted waveguide filters for use in communications systems," in *G-MTT Int. Microwave Symp. Dig.*, May 1969, pp 291–297.

[8] A.E. Williams, W.G. Bush, and R.R. Bonetti, "Predistortion technique for multicoupled resonator filters," *IEEE Trans. Microwave Theory Tech.*, vol. MTT-33, no. 5, pp. 402–407, May 1985.

[9] V. Miraftab and M. Yu, "Generalized lossy microwave filter synthesis and design," in *Proc. IEEE MTT-S Int. Microwave Symp., Atlanta*, GA, June 2008.

[10] M. Yu and V. Miraftab, "Cavity microwave filter assembly with lossy networks," patent pending.